Optical-absorption spectrum of a one-dimensional strong-coupling Coulombic Hubbard exciton

J.-P. Gallinar
Departamento de Física, Universidad Simón Bolívar, Apartado 89000, Caracas 1080A, Venezuela
(Received 17 February 1993)

We obtain the optical-absorption spectrum associated with an electron and a hole which attract each other according to the Coulomb law within a strong-coupling generalized half-filled Hubbard-band chain. We find a continuous absorption band characterized by a Lifshitz tail-edge singularity, and penetrated in a resonant manner by an infinite number of localized absorption bands. A comparison is made with the continuum (or effective-mass approximation) limit of the theory. Finally, a formal expression is also presented for the case of a quite arbitrary law of electron-hole interaction within the Hubbard chain, while in the presence of a constant electric field.

I. INTRODUCTION

Within the context of the simple Hubbard Hamiltonian[1] we developed a theory,[2] some time ago, to describe the optical-absorption spectrum associated with a half-filled strong-coupling ($U\rightarrow\infty$) antiferromagnetic Hubbard-band chain.[2] In subsequent works,[3–6] various aspects of this interesting theory[2] were elucidated, and extended to include, among other things, mainly the possible effects of nearest neighbors,[4–6] or even longer-ranged[5,6] interelectronic interactions. The latter, within the framework of the Wigner lattice theory, were proposed by Hubbard[7,8] in 1978 for some of the TCNQ (tetracyanoquinodimethane) salts. More recently,[9] Wannier-Stark ladders in the presence of a constant electric field have also been considered[9] in the optical-absorption spectrum of our Hubbard-band exciton theory.[2] They have been shown[9] to modify the spectrum in a strikingly complex manner.

Yet, a more complete solution has not been given as an application of this theoretical formalism.[2] This we do here, and in Sec. II a formal continued fraction expression is presented for the absorption spectrum of the "Hubbard exciton." This expression is appropriate for a quite *arbitrary* law of electron and hole attraction, similar to that proposed by Hubbard[7,8] in his generalized Hamiltonian and Wigner lattice theory,[7,8] but it may include the effects of a constant electric field.

Then, in Sec. III this formal expression is applied to the important theoretical case of a Coulombic[10–12] law of attraction within the electron-hole pair. After studying diverse results pertaining to the Coulombic law and its integrated intensity bands of absorption, a brief comparison is made with the continuum (or effective-mass approximation) limit, associated to Wannier-like Coulombic excitons. Some conclusions are given in Sec. IV, and an Appendix explains at length mathematical details pertaining to the Coulomb problem on a lattice.[10–12]

II. CONTINUED FRACTION EXPRESSION

We consider Hubbard's[7,8] generalized Hamiltonian on a linear chain, with a constant electric field E superimposed along the chain direction, as[9]

$$H=-t\sum_{j,\sigma,\delta=\pm1}c^{\dagger}_{j+\delta,\sigma}c_{j,\sigma}+U\sum_{j}n_{j\uparrow}n_{j\downarrow}+\tfrac{1}{2}\sum_{i\neq j}V_{|i-j|}n_in_j+\alpha\sum_j jn_j\ , \tag{2.1}$$

where $c^{\dagger}_{j,\sigma}$ ($c_{j,\sigma}$) is the creation (destruction) operator for an electron of spin σ in the Wannier state localized at site j, and $n_{j\sigma}=c^{\dagger}_{j,\sigma}c_{j,\sigma}$ is the occupation number of this state. The total number of electrons at site j is given by the operator $n_j=\sum_\sigma n_{j\sigma}$, and t is the transfer integral (or hopping matrix element) between nearest-neighbor sites; U is the repulsion energy of two electrons on the same site, and $V_{|i-j|}\equiv V_n=V_{-n}$ is the repulsion energy of two electrons on nth-nearest-neighbor sites; $\alpha\equiv|e|Ea$, where e is the electronic charge and a is the lattice constant. The above is the Hamiltonian proposed by Hubbard[7,8] (with $\alpha=0$) in his Wigner lattice theory for some TCNQ salts; in particular, Hubbard tried to describe diverse aspects of the optical spectra of some of the charge-transfer salts of TCNQ in terms of the above Hamiltonian with $U\rightarrow\infty$.

If we consider the Wigner lattice for the half-filled band, as shown in Fig. 1, with $U\rightarrow\infty$, we see that charge-transfer absorption occurs when an electron is made to "jump" to a nearest-neighbor site [Fig. 1(a)], thereby creating a doubly occupied site and an adjacent hole. For this to be possible, the two original adjacent electrons in the chain must have their spins in opposite directions. The optical frequency for this absorption is roughly $U-V_1\pm\alpha$ [depending upon whether the exciton dipole moment is antiparallel (+), or parallel (−) to E]. Once the doubly occupied site (or "electron") has been created, it and the hole can obviously propagate irrespective of the spin configuration of the rest of the chain. Thus, when the electron and the hole are nth nearest neighbors of each other, the energy of the excited configuration is $\approx U-V_n\pm n\alpha$, as pictured in Fig. 1(b). After a straightforward extension of our theory,[2,6] one finds the real part $\sigma_R(\omega)$ of the conductivity to be given by[9]

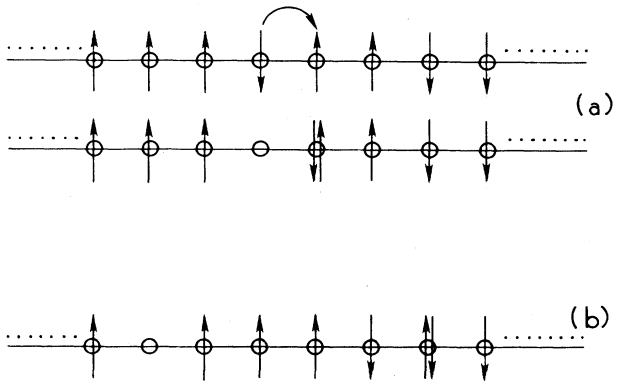

FIG. 1. (a) Creation of the Hubbard exciton in the half-filled ($U\to\infty$) generalized Hubbard chain. The circles represent the lattice sites where the localized spins reside, represented by the arrows; (b) doubly occupied site (or "electron") and hole are moved five lattice constants away from each other, and some of the spins in (a) are thereby reversed by the motion.

$$\sigma_R(\omega)=\frac{2N\pi e^2a^2t^2p}{U\Omega}\int_0^1 dx\, Q(x,\beta)\rho(\omega;x)\ , \tag{2.2}$$

where N, Ω, and p are the number of lattice sites, the volume of the sample, and the probability of the initial electron-hole pair creation ("Hubbard exciton"), respectively. We have

$$\rho(\omega;x)\equiv[\rho_+(\omega;x)+\rho_-(\omega;x)]/2$$

and

$$\rho_\pm(\omega;x)\equiv\frac{1}{\pi}\mathrm{Im}\left\{z+V_1\pm\alpha - \frac{(2tx)^2}{z+V_2\pm2\alpha-\dfrac{(2tx)^2}{z+V_3\pm3\alpha-\cdots}}\right\}^{-1}, \tag{2.3}$$

with $z\equiv\omega-U-i0^+$. The terms $\rho_-(\omega;x)$ and $\rho_+(\omega;x)$, respectively, correspond to the antiparallel and parallel alignment of the exciton dipole moment with the electric field E. The function $Q(x,\beta)$ weighs the density of states $\rho(\omega;x)$, and is given for a uniform lattice by[2,3]

$$Q(x,\beta)=\frac{2\cos\beta}{\pi(1-x^2\sin^2\beta)\sqrt{1-x^2}}\ , \tag{2.4}$$

where the angle β $(0\le\beta\le\pi/2)$ is defined by $p\equiv\tan^2(\beta/2)$. For a "perfectly" antiferromagnetic spin arrangement of the electrons in the Wigner chain we have $p=1$, while for a random or a ferromagnetic spin arrangement $p=\frac{1}{2}$ and 0, respectively. The factor U^{-1} in (2.2) ensures that the optical absorption vanishes in the limit $U\to\infty$. This is as it should be for a half-filled band, and (2.2) is an asymptotical expression for the vanishing of our absorption spectrum $\sigma_R(\omega)$ in the strong-coupling limit $U\to\infty$ of the theory. Thus, Eq. (2.2) above gives the general line shape in our theory for $U\to\infty$; the other parameters (t, the V_n's, and the electric field E) being finite, but otherwise quite unrestricted (although $t\ll U$, and $V_n\ll U$). In consequence (2.2) addresses itself to the solution, for the half-filled band, of part of the problem posed by Hubbard[7,8] in his Wigner lattice theory for optical absorption, namely, the improvement, upon the $t=0$ treatment presented there,[7,8] of the study of band-motion effects upon the optical absorption.

Two mathematically distinct cases arise in the treatment of the general solution in (2.2) when $\alpha=0$.

(a) If V_n is such that it vanishes for $n>k$, then the density of states $\rho(\omega;x)$ has a "continuous" part $\rho_c(\omega;x)$ that can be shown[13] to be of the form

$$\rho_c(\omega;x)=\frac{\sqrt{(4tx)^2-(\omega-U)^2}}{\mathcal{P}(\omega-U;tx,V_1,V_2,\ldots,V_k)}\ , \tag{2.5}$$

where $\mathcal{P}(\omega-U;tx,V_1,V_2,\ldots,V_k)$ is a polynomial in $(\omega-U)$ of degree $2k-1$, and a rational function of the other variables.[14] Because of this, the "continuous" or extended absorption spectrum associated to (2.2) can very remarkably be expressed always in terms of the three complete elliptical integrals, though in an increasingly complex manner as k increases. The real simple zeros in $(\omega-U)$ of the polynomial of degree $2k-1$ in (2.5) can easily be found numerically, and shown to give rise in general to a corresponding number of localized absorption bands when substituted back into the quadrature expressed in (2.2). For $k=1$ a completely analytical solution exists,[9] and for $k>1$ this may also be possible for special values of the parameters.

(b) The potential V_n is of infinite range. As an idealized description of this case, for which we have found an analytical solution, we shall take $V_n=V/n$, (2.6), i.e., a Coulomb potential attraction between the electron and hole in the Hubbard exciton. Although (2.6) cannot, of course, be expected to hold experimentally in any "exact" manner, we surmise that it should contain relevant physics as pertains to the optical-absorption spectrum of the "Hubbard exciton." Theoretically it is certainly of mathematical interest in itself, since it involves the solution of a Coulomb potential problem on a lattice.[10–12]

III. COULOMBIC HUBBARD EXCITON

By substituting (2.6) into (2.3) (with $\alpha=0$), and calculating the value of the infinite continued fraction, after an interesting piece of mathematics (see Appendix), we find for $\sigma_R(\omega)$ the following expression: $\sigma_R(\omega)=\sigma_c(\omega)+\sigma_L(\omega)$, where the continuous or extended absorption line shape $\sigma_c(\omega)$ is given by

$$\sigma_c(\omega)=\frac{e^2a^2tNp|v|}{\Omega U}\times\int_0^1 dx\frac{u(1-|k'|)u(x-|k'|)(\cos\beta)\Phi(x)}{x^2(1-x^2\sin^2\beta)\sqrt{1-x^2}} \tag{3.1}$$

where

$$\Phi(x)\equiv\frac{\exp[-(|v|/\sqrt{x^2-k'^2})\arcsin(k'/x)]}{\sinh(\pi|v|/2\sqrt{x^2-k'^2})},$$

with $v\equiv V/2t$, $k'\equiv(\omega-U)/4t$, and $u(y)$ the unit step function. The localized or discrete absorption bands which arise from the bound eigenvalues of the Coulomb potential are given by

$$\sigma_L(\omega)=\frac{e^2a^2tNp|v|^3\cos\beta}{2\Omega U}\sum_{n=1}^{\infty}L_n(k';v,\beta), \tag{3.2}$$

with $L_n(k';v,\beta)$ expressed through

$$L_n(k';v,\beta)\equiv\left[\frac{|k'|-|k'|_{\min,n}}{|k'|+|k'|_{\min,n}}\right]^{n-1}u(1-x_n)u(-k')\frac{1}{n^3[1-(k'^2-k'^2_{\min,n})\sin^2\beta]}\times\frac{1}{[|k'|+|k'|_{\min,n}]^2\sqrt{k'^2-k'^2_{\min,n}}\sqrt{k'^2_{\max,n}-k'^2}} \tag{3.3}$$

with $|k'|_{\min,n}\equiv|v|/2n$, $|k'|_{\max,n}\equiv\sqrt{1+k'^2_{\min,n}}$, and $x_n\equiv(k'^2-k'^2_{\min,n})^{1/2}$. The unit step functions in (3.3) imply, for the corresponding nth term in the series, the following condition on k': $-|k'|_{\max,n}\le k'\le-|k'|_{\min,n}$. The spectrum $\sigma_R(\omega)$ is shown in Figs. 2–4 for some selected values of v and β. As v is turned on, there appear an infinite number $n=1,2,3,\ldots$, of localized absorption bands which extend in all from $k'=-\sqrt{1+(v/2)^2}$ up to $k'=0$, with diminishing intensities as $n\to\infty$. The band for $n=1$ behaves differently from the others: it diverges at both $k'=-|k'|_{\max,1}$ and at $k'=-|k'|_{\min,1}=-|v|/2$, while for $n>1$, the absorption bands diverge only at $k'=-|k'|_{\max,n}$, and tend to zero when $k'\to-|k'|_{\min,n}$. The continuous $\sigma_c(\omega)$ absorption band in (3.1) which exists in the interval $-1\le k'\le1$ has been calculated through Gaussian integration. It is penetrated in a "resonant" manner by the localized absorption bands in the region $-1\le k'\le0$; and as $|v|$ increases up to $|v|=2$, the $n=1$ band square-root divergence at $k'=-|v|/2$ moves to the left, until for $|v|=2$ it hits the $-|k'|_{\max,\infty}$ divergence at $k'=-1$. This is shown in Fig. 2 for the ferromagnetic spin arrangement ($p=0$) by the confluence of the two infinities at $k'=-1$. As $|v|$ is further increased beyond $|v|=2$, the $-|k'|_{\min,1}$ divergence continues its "sweep" to the left, until at the critical value $|k'|_{\min,1}=|k'|_{\max,2}$, or $|v|=4/\sqrt{3}\cong2.31$, the $n=1$ and 2 bands first disentangle from each other. This is shown in Fig. 3 for $|v|=3$, where the $n=1$ and 2 $\sigma_L(\omega)$ bands are clearly separated by an interval of null spectrum. In this same Fig. 3, the extended or continuous absorption band $\sigma_c(\omega)$ also clearly shows, for $k'\to1$, a Lifshitz[15] tail-edge singularity present in the integral in (3.1); in this region the absorption is exponentially vanishing. As $|v|$ increases from zero, the $\sigma_L(\omega)$ bands become narrower and the intensity of the spectrum monotonically leaks into the $n=1$ band, while going through a maximum for the other ($n>1$) bands at corresponding values of $|v_0|_n$ (see Fig. 5 for $p=1$). Also, as p approaches $p=1$—the value of p for a completely ordered antiferromagnetic arrangement of the spin of the electrons in the Wigner lattice in Fig. 1(a)—the $\sigma_L(\omega)$ bands become *effectively* narrower, with most of their intensity localized around the divergences at $k'=-|k'|_{\max,n}$. This is shown in Fig. 3 for $p=0.97$ for the bands $n=1,2,3$, where we notice that for $n=1$ the divergence at $k'=-|k'|_{\min,1}$ has *effectively* disappeared. In Fig. 4 we exhibit the spectrum for (exactly) $p=1$ ($\beta=\pi/2$) with the $\sigma_L(\omega)$ bands (shown for $|v|=3$, only) collapsed into

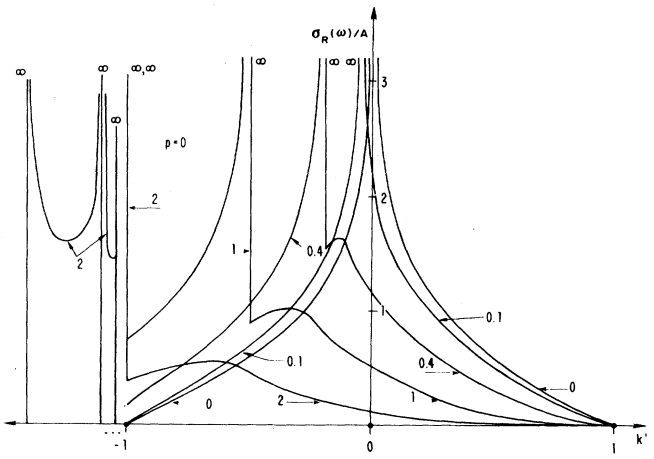

FIG. 2. Plot of $\sigma_R(\omega)/A$ (with $A\equiv e^2a^2tpN/\Omega U$) vs $k'\equiv(\omega-U)/4t$ is shown for several values of $v\equiv V/2t$, for a perfect ferromagnetic ($p=0$) arrangement of the spins of Fig. 1(a). Except for $v=2$, only the region $|k'|\le1$ is actually displayed for visual convenience.

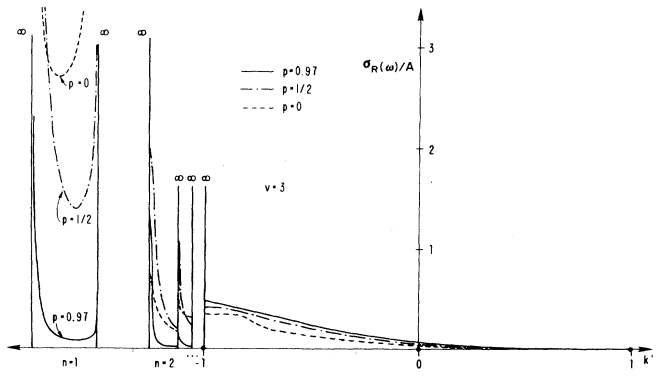

FIG. 3. Plot of $\sigma_R(\omega)/A$ vs k' for $v=3$ and several values of p. For this value of v, the spectrum vanishes in an interval between the $n=1$ and 2 localized absorption bands.

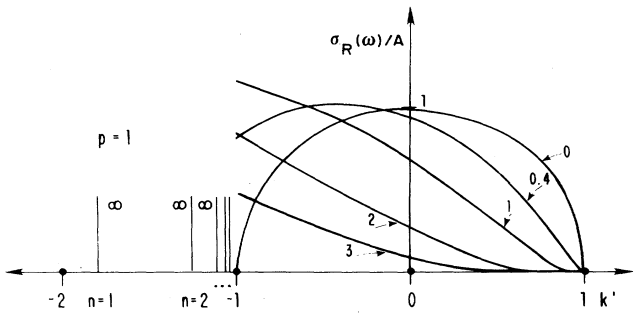

FIG. 4. Plot of $\sigma_R(\omega)/A$ vs k' is shown for several values of v, for a perfect antiferromagnetic ($p=1$) spin arrangement. Except for $v=3$, only the region $|k'|\leq 1$ is actually displayed for visual convenience. The localized absorption peaks shown (for $v=3$) represent Dirac δ functions, schematically drawn to an arbitrary height scale. Notice the hydrogeniclike ($\sim 1/n^2$) accumulation of these peaks close to $k'\simeq -1$ for $n\to\infty$.

δ-function peaks. These peaks, as $n\to\infty$, show a typical $1/n^2$ hydrogeniclike accumulation close to $k'=-1$. It is then a simple matter (see Appendix) to prove that at $k'=-1$, the $\sigma_L(\omega)$ and $\sigma_c(\omega)$ spectra join continuously at a common value of $A\pi|v|\exp(-|v|)$, with $A\equiv e^2a^2tpN/U\Omega$. Furthermore, the intensity I_n^L under the nth $\sigma_L(\omega)$ band (shown in Fig. 5) is then given (for $p=1$) by

$$I_n^L(v)\equiv\int[\sigma_L(\omega)]_n d\omega=2\pi At\frac{\dot{J}_n^{n-1}(1-\dot{J}_n)^3}{1+\dot{J}_n}\ , \tag{3.4}$$

with

$$\dot{J}_n(v)\equiv\frac{|k'|_{\max,n}-|k'|_{\min,n}}{|k'|_{\max,n}+|k'|_{\min,n}}\ .$$

For $n>1$, the function $I_n^L(v)$ has a relative maximum at $|v_0|_n=n[f(n)-f^{-1}(n)]$, where

$$f(n)\equiv\left[\frac{n+1}{\sqrt{n^2+3}-2}\right]^{1/2}\ .$$

The point $|v_0|_n$ at which the relative maximum of $I_n^L(v)$ occurs is a rather insensitive function of n; varying from $|v_0|_2\cong 3.38$ down to $|v_0|_\infty=3$.

Although $I_n^L(v)$, given by (3.4) for a general n, varies in a complicated manner upon n, it does obey for $n\to\infty$ the simple asymptotic $1/n^3$ relation characteristic for the oscillator strength of Coulombic Wannier excitons. So does the law $k_n'=-\sqrt{1+(v/2n)^2}$, for the bound "eigenvalues" of the Coulomb potential problem on a lattice[10-12] (see Appendix and Fig. 4), which displays a typical $1/n^2$ hydrogenic accumulation close to the edge of the continuous spectrum $\sigma_c(\omega)$ at $k'_\infty=-1$. Thus we expect that for $n\to\infty$ (i.e., for a loosely bound or large "Hubbard exciton") we shall recover some of the usual results of the continuum (or effective-mass approximation) limit of the theory for Wannier excitons.

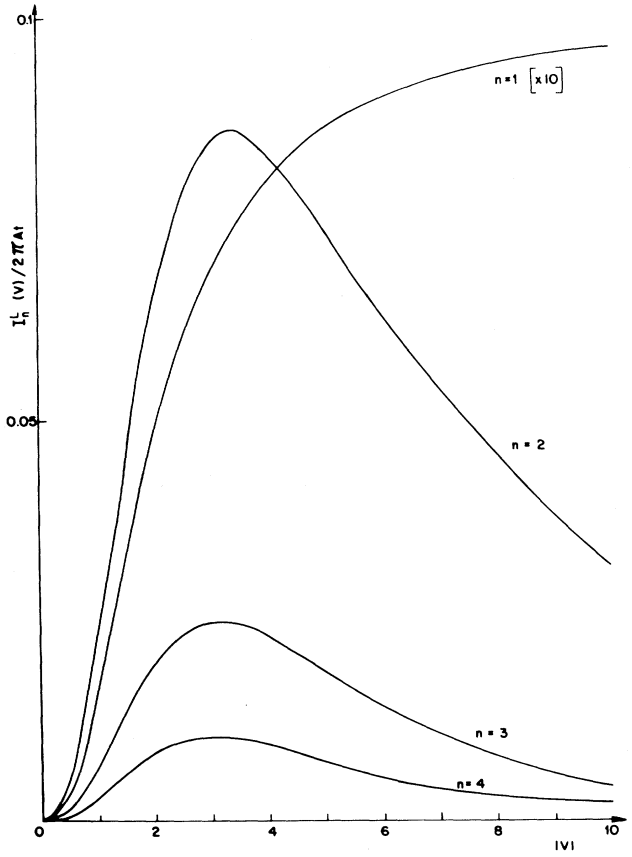

FIG. 5. Plot of $I_n^L(v)/2\pi At$ vs $|v|$ for an antiferromagnetic ($p=1$) spin arrangement. For $|v|\to\infty$ all curves with $n\geq 2$ go to zero, while the $n=1$ curve saturates to one. For $n\geq 2$, $|v_0|_n$, the position of the maximum, depends weakly upon n, and for a given $|v|$ these curves go roughly as $1/n^3$.

IV. CONCLUSIONS

We have presented a formal solution to the problem originally posed by us[2] for the optical-absorption spectrum of the strong-coupling half-filled generalized Hubbard chain. Our solution addresses itself to part of the problem posed by Hubbard[7,8] concerning the need for a more precise treatment of the band-motion effects on his[7] Wigner lattice theory for optical absorption. In fact, in our Eq. (2.2) the band-motion energy $\approx t$ can be arbitrary as compared with the V_n's energies. Here, it must be emphasized that our[2] theory applies to the half-filled band (and *only* to it), so that upon the "frozen" Wigner lattice for $U\to\infty$, band-motion effects can be grafted on in a relatively simple manner, in sharp contrast, then, with the Wigner lattice for a general band filling or electron density as considered by Hubbard.[7,8]

Our solution, applied to the Coulomb potential, reveals a complex and rich excitonic optical spectrum, some of whose features might, in principle, be experimentally observable.[16] In fact, some authors like Yakushi, Kusaka, and Kuroda[16] have analyzed the (infrared) optical absorption of K-TCNQ (potassium tetracyanoquinodimethane) in terms of our theory with *only* nearest-neighbor electronic repulsion V_1. Jacobsen, Johannsen, and Bechgaard[16] have also interpreted the infrared ab-

sorption of DBTSF-TCNQF$_4$ (dibenzotetraselenafulvalene-tetrafluoro-TCNQ) analogously. In both cases,[16] the salient experimental feature of an asymmetric (continuous) spectrum with a maximum shifted downwards in frequency agreed well with our theoretical predictions. In the present work with a Coulomb interaction, this theoretical feature is also present (as can be seen in our Figs. 2–4), but new ones manifest themselves, too. In particular, the characteristic Lifshitz edge singularity (see Appendix) with exponentially vanishing absorption in these same figures implies not only a shorter effective absorption width, but also one with zero slope at the upper edge. This is a characteristic edge singularity of the spectrum which arises from the Coulomb interaction,[10] while being absent otherwise. Also present only here is the infinite number ($n=1,2,3,\ldots$) of localized absorption peaks, arising from the bound eigenvalues of the Coulomb potential.

Of course, one must bear in mind that some of these predicted effects might be masked by the screening[7,17] of the electronic interactions in some of the half-filled-band linear materials (organic or otherwise) to which our theory[2] might apply. To the extent that screening has been argued to be rather ineffective[17] (especially the short-range one) for the exactly half-filled-band organic compounds,[17] one might envisage the suitability of our present results.

Finally, we have solved a Coulomb potential problem on a "lattice,"[10–12] and have also laid the groundwork for the further study of the electric Stark effect[9] upon the absorption spectrum of our Coulombic "Hubbard exciton."

ACKNOWLEDGMENT

The support of this research by CONICIT's SPI Scholarship No. 0244 is gratefully acknowledged.

APPENDIX

In this appendix we evaluate the continued fraction that appears in (2.3), for $\alpha=0$ and $V_n=V/n$, as well as deriving (3.1) and (3.2) in the text. Finally, we show (for $p=1$) that the spectra $\sigma_c(\omega)$ and $\sigma_L(\omega)$ join "continuously" at $k'=-1$, with a common value of $A\pi|v|\exp(-|v|)$.

We can write $\rho(\omega;x)\equiv(1/\pi)\mathrm{Im}G(z)$ with

$$G(z)\equiv\cfrac{1}{z+V-\cfrac{(2tx)^2}{z+\cfrac{V}{2}-\cfrac{(2tx)^2}{z+\cfrac{V}{3}-\cdots}}}\ , \tag{A1}$$

where[18] we have

$$G(z)=\lim_{n\to\infty}A_n/B_n\ . \tag{A2}$$

A_n is given by a second-order linear difference equation, namely (for $n\geq 1$),

$$A_{n+1}+(2tx)^2A_{n-1}=\left[z+\frac{V}{n+1}\right]A_n\ , \tag{A3}$$

with $A_0=0$ and $A_1=1$, while B_n satisfies (A3) also, but with initial conditions $B_0=1$ and $B_1=z+V$. Thus

$$G(z)=a_1/b_1\ , \tag{A4}$$

where a_1 and b_1 are to be adjusted to satisfy the previous initial conditions for A_n and B_n, in the linear combinations

$$\begin{aligned}A_n&=a_1\theta_1(n)+a_2\theta_2(n)\ ,\\ B_n&=b_1\theta_1(n)+b_2\theta_2(n)\ .\end{aligned} \tag{A5}$$

In (A5), $\theta_1(n)$ and $\theta_2(n)$ are linearly independent[19] solutions of (A3), with $\theta_1(n)$ the dominant one when $n\to\infty$. Solving for a_1 and b_1 from (A5), we find that

$$G(z)=\frac{1}{z+V-[\theta_2(1)/\theta_2(0)]}\ . \tag{A6}$$

Although a_2 and b_2 in the linear combinations in (A5) also have to be adjusted, they do not appear in (A4) for $G(z)$. By standard methods,[19] the two linearly independent solutions of (A3) can be taken to be

$$\theta_1(n)=\frac{x_1^{n+1-k}\Gamma(n+2)\Gamma(1-k)}{x_2^{1-k}\Gamma(n+2-k)}\times F(1-k,n+2,n+2-k;x_1/x_2)$$

and

$$\theta_2(n)=\frac{x_2^{n+1-k}\Gamma(n+2)\Gamma(1+k)}{x_1^{1+k}\Gamma(n+2+k)}\times F(1+k,n+2,n+2+k;x_2/x_1)\ , \tag{A7}$$

where $k\equiv V/(x_1-x_2)$; and

$$x_{1,2}=[z\pm\sqrt{z^2-(4tx)^2}]/2$$

are the roots of the quadratic equation in X, namely, $X^2-zX+(2tx)^2=0$. The functions $F(a,b,c;Z)$ and $\Gamma(z)$ are the hypergeometric and gamma functions, respectively. Substituting $\theta_2(1)$ and $\theta_2(0)$ from (A7) into (A6), one finds

$$G(z)=\frac{1}{z+V-(2x_2/2+k)\{F(1+k,3,3+k;x_2/x_1)/F(1+k,2,2+k;x_2/x_1)\}}\ , \tag{A8}$$

where the function in $\{\}$ in the denominator of (A8), being of the form $F(a,b,c;Z)/F(a,b-1,c-1;Z)$, represents the so-called continued fraction of Gauss.[20] After some algebra involving Gauss's relations for the "contiguous"[20] functions of the hypergeometric function, (A8) can be simplified to

$$G(z)=\frac{1}{x_1}-\frac{VF(1+k,1,2+k;x_2/x_1)}{x_1^2(1+k)}=\frac{1}{x_1}-V\left[\frac{x_1^{k-1}}{x_2^{k+1}}\right]B_{(x_2/x_1)}(1+k,0)\ , \tag{A9}$$

where $F(1+k,1,2+k;x_2/x_1)$ has been expressed in terms of the incomplete beta function[20] $B_x(a,b)$, through the relationship[20] $B_x(a,b)=a^{-1}x^aF(a,1-b,a+1;x)$. To find $\rho(\omega;x)$, we consider first the case $|z|\le 4tx$, and write that $\rho(\omega;x)=[G(z)-G(\bar{z})]/2\pi i$, where $z\equiv\omega-U-i0^+$, and $\bar{z}$ is the complex conjugate. If $|z|<4tx$, k becomes pure imaginary and $\bar{k}=-k$, with $\bar{x}_1=x_2$ and $\bar{x}_2=x_1$. Thus

$$\rho(\omega;x)=\frac{1}{2\pi i x_1x_2}\left\{x_2-x_1-V\left[\frac{x_2F(1+k,1,2+k;x_2/x_1)}{x_1(1+k)}-\frac{x_1F(1-k,1,2-k;x_1/x_2)}{x_2(1-k)}\right]\right\} \tag{A10}$$

for $|z|\le 4tx$. Very remarkably, (A10) can be found in terms of elementary transcendental functions *only*. To show this, we express both of the hypergeometric functions that appear in (A10) in terms of $F(k,1,1+k;x_2/x_1)$, and find, using the "contiguous" hypergeometric functions,[20] that

$$F(1+k,1,2+k;x_2/x_1)=\frac{x_1(1+k)}{kx_2}[F(k,1,1+k;x_2/x_1)-1]\ , \tag{A11}$$

while

$$F(1-k,1,2-k;x_1/x_2)=k(k-1)\Gamma(k)\Gamma(-k)\left[-\frac{x_1}{x_2}\right]^{k-1}+\frac{x_2(1-k)}{kx_1}F(k,1,1+k;x_2/x_1)\ . \tag{A12}$$

Substituting (A11) and (A12) into (A10), there results

$$\rho(\omega;x)=\frac{kV}{2\pi i x_1x_2}\Gamma(k)\Gamma(-k)\left[-\frac{x_1}{x_2}\right]^k\ , \tag{A13}$$

remarkably independent of the hypergeometric function. After some algebraic simplifications, and noting that x_1/x_2 is a complex number on the unit circle, (A13) finally leads to

$$\rho(\omega;x)=\frac{V}{(2tx)^2}\left\{\exp\left[\frac{2V\cos^{-1}(-z/4tx)}{\sqrt{(4tx)^2-z^2}}\right]-\exp\left[\frac{-2V\cos^{-1}(z/4tx)}{\sqrt{(4tx)^2-z^2}}\right]\right\}^{-1} \tag{A14}$$

for $|z|\le 4tx$. To obtain (A14) from (A13), use has been made of the relationship[20]

$$\Gamma(iy)\Gamma(-iy)=\pi/y\sinh(\pi y)\ ,$$

valid for the gamma function. We turn now to the case $|z|>4tx$. Here we write in (A9) that[20]

$$\frac{F(1+k,1,2+k;x_2/x_1)}{1+k}=\sum_{n=0}^{\infty}\frac{(x_2/x_1)^n}{1+k+n}\ ,$$

and find, after algebraic manipulations, that

$$\rho(\omega;x)=\frac{|V|^3}{x_1^2}\sum_{n=0}^{\infty}\frac{(x_2/x_1)^n}{(1+n)^2}\times\frac{\delta(z+\sqrt{(4tx)^2+V^2/(1+n)^2})}{\sqrt{(4tx)^2(1+n)^2+V^2}}\ . \tag{A15}$$

In (A15), x_1 and x_2 have to be evaluated according to the Dirac δ functions which appear therein. Doing so, one finally finds for $|z|>4tx$ that

$$\rho(\omega;x)=\sum_{n=0}^{\infty}\frac{\alpha_n^n(1-\alpha_n)^3}{1+\alpha_n}\delta(z+\sqrt{(4tx)^2+V^2/(1+n)^2})\ , \tag{A16}$$

with

$$\alpha_n\equiv\frac{\sqrt{(4tx)^2+V^2/(1+n)^2}-V/(1+n)}{\sqrt{(4tx)^2+V^2/(1+n)^2}+V/(1+n)}\ .$$

To obtain (3.1) we substitute (A14) into (2.2), and make use of the formulas $\sin^{-1}y=\cos^{-1}(-y)-(\pi/2)=(\pi/2)-\cos^{-1}y$, in (A14). To obtain (3.2) we substitute instead (A16) into (2.2) and find

$$\frac{\sigma_L(\omega)}{\bar{K}}=\sum_{n=0}^{\infty}\int_0^1 dx\ Q(x,\beta)\frac{\alpha_n^n(1-\alpha_n)^3}{1+\alpha_n}\delta(\varphi_n(x))\ ,$$

where

$$\bar{K}\equiv\frac{2\pi e^2a^2t^2Np}{\Omega U}\ ,$$

and

$$\varphi_n(x)\equiv\omega-U+\sqrt{(4tx)^2+V^2/(1+n)^2}\ .$$

Using the properties of Dirac's δ function, $\sigma_L(\omega)$ can be written as

$$\frac{\sigma_L(\omega)}{\bar{K}}=\sum_{n=0}^{\infty}\sum_i Q(x_i,\beta)\left[\frac{\alpha_n^n(1-\alpha_n)^3}{1+\alpha_n}\right]_{x_i}\left|\frac{d\varphi_n}{dx}\right|^{-1}_{x=x_i},$$

with the $x_i(\omega)$ being those simple roots of the equation $\varphi_n(x)=0$ that satisfy $0\le x_i\le 1$. We find (after relabelling, $i\leftrightarrow n$), that

$$x_n(\omega)=\sqrt{k'^2-(V/2(n+1))^2}\ ,$$

with $k'\equiv(\omega-U)/4t$, and $v\equiv V/2t$. Furthermore,

$$\alpha_n(x_n)=\frac{2(n+1)|k'|-|v|}{2(n+1)|k'|+|v|}$$

for $k'\le 0$. After some manipulations, we obtain for $\sigma_L(\omega)$ that

$$\frac{\sigma_L(\omega)}{\bar{K}}=\frac{|v|^3}{2t}\sum_{n=0}^{\infty}\frac{Q(x_n,\beta)u(1-x_n)\alpha_n^n(x_n)}{(n+1)[2(n+1)|k'|+|v|]^2\sqrt{k'^2-[v/2(n+1)]^2}}\ , \tag{A17}$$

with $u(y)$ the unit step function, and k' in each term of the series restricted to the interval

$$-\left[1+\left[\frac{v}{2(n+1)}\right]^2\right]^{1/2}\le k'\le-\frac{|v|}{2(n+1)}\ .$$

Finally, by inserting the value of $Q(x_n,\beta)$ in (A17), defining

$$|k'|_{\min,n}\equiv\frac{|v|}{2n}\ ,\quad |k'|_{\max,n}\equiv\sqrt{1+|k'|^2_{\min,n}}\ ,$$

and some additional manipulations, we obtain (3.2) in the text.

To conclude this appendix, we now show that $\sigma_c(\omega)$ and $\sigma_L(\omega)$ join smoothly (up to higher-order derivatives) for $p=1$, at $k'=-1$. First, we show that (A14) and (A16) do so for $x=1$. In effect, from (A14) we obtain (setting $x=1$) that

$$\lim_{k'_+\to-1}\rho(k';1)=\frac{V}{(2t)^2}\exp\left[-\frac{V}{2t}\psi\right]$$
$$=\frac{V}{(2t)^2}\exp\left[-\frac{V}{2t}\right],$$

where

$$\psi\equiv\lim_{k'_+\to-1}\frac{\cos^{-1}(-k')}{\sqrt{1-k'^2}}=1\ .$$

On the other hand, we will have that, as an interesting aside, $\rho(k';1)$ behaves for $k'\to1$ as

$$\rho(k';1)\xrightarrow[k'\to1]{}\frac{V}{(2t)^2}\exp\left[-\frac{\pi V}{2t\sqrt{1-k'^2}}\right],$$

i.e., in the form of a Lifshitz[15] tail-edge singularity. Thus, for $k'=1$, $\rho(k';1)$ and *all* its derivatives vanish for any $V\neq0$. Let us turn now to (A16). Here, we will have

$$\lim_{k'_-\to-1}\rho(k';1)=\lim_{n\to\infty}\frac{\alpha_n^n(1-\alpha_n)^3}{1+\alpha_n}\left|\frac{\partial\omega(n)}{\partial n}\right|^{-1}, \tag{A18}$$

where

$$\omega(n)\equiv-\sqrt{(4t)^2+V^2/(n+1)^2}\ .$$

But, since

$$\lim_{n\to\infty}(1-\alpha_n)\cong\frac{V}{2t(n+1)}\ ,$$

we have $\lim_{n\to\infty}\alpha_n^n=\exp(-V/2t)$.

Thus in (A18) we obtain

$$\lim_{k'_-\to-1}\rho(k';1)=\exp\left[-\frac{V}{2t}\right]\lim_{n\to\infty}\left[\frac{1}{2}\right]\left[\frac{V}{2t(n+1)}\right]^3\left|\frac{V^2}{[(4t)^2+V^2/(n+1)^2]^{1/2}(n+1)^3}\right|^{-1}$$
$$=\frac{V}{(2t)^2}\exp\left[-\frac{V}{2t}\right],$$

Q.E.D. The common value of the spectrum at $k'=-1$ can easily be found from (2.2) for $p=1$. Here, we have[3] that $Q(x,\pi/2)=\delta(x-1)$, and consequently,

$$\sigma_R(k'=-1)=\frac{2N\pi e^2a^2t^2}{U\Omega}\int_0^1 dx\ Q(x,\pi/2)\rho(k'=-1;x)$$
$$=2\pi At\rho(k'=-1;1)=A\pi|v|\exp(-|v|)\ .$$

[1]J. Hubbard, Proc. R. Soc. London Ser. A **276**, 238 (1963); **281**, 401 (1965).
[2]S. K. Lyo and J.-P. Gallinar, J. Phys. C **10**, 1693 (1977), and references therein.
[3]J.-P. Gallinar, Phys. Rev. B **17**, 807 (1978).
[4]S. K. Lyo, Phys. Rev. B **18**, 1854 (1978).
[5]J.-P. Gallinar, in *Quasi-One-Dimensional Conductors II,* edited by S. Barišić, A. Bjeliš, J. R. Cooper, and B. Leontić, Springer Lecture Notes in Physics Vol. 96 (Springer, Berlin, 1979), p. 105.
[6]J.-P. Gallinar, Phys. Lett. **70A**, 353 (1979); J. Phys. C **12**, L335 (1979).
[7]J. Hubbard, Phys. Rev. B **17**, 494 (1978).
[8]J. Hubbard, in *Quasi-One-Dimensional Conductors II* (Ref. 5), p. 11.
[9]E. R. Chalbaud and J.-P. Gallinar, J. Phys. Condens. Matter **1**, 3325 (1989).
[10]J.-P. Gallinar, Phys. Lett. **103A**, 72 (1984).
[11]D. C. Mattis, Rev. Mod. Phys. **58**, 361 (1986).
[12]A. A. Kvitsinsky, J. Phys. A **25**, 65 (1992).
[13]J.-P. Gallinar (unpublished).
[14]If all V_n's are zero, then $\mathcal{P}(\omega-U;tx)$ is of zero degree in $(\omega-U)$.
[15]I. M. Lifshitz, Adv. Phys. **13**, 483 (1969).
[16]K. Yakushi, T. Kusaka, and H. Kuroda, Chem. Phys. Lett. **68**, 139 (1979); C. S. Jacobsen, Ib Johannsen, and K. Bechgaard, Phys. Rev. Lett. **53**, 194 (1984).
[17]S. Mazumdar and A. N. Bloch, Phys. Rev. Lett. **50**, 207 (1983); S. Mazumdar and Z. G. Soos, Phys. Rev. B **23**, 2810 (1981).
[18]G. A. Baker, Jr., *Essentials of Padé Approximants* (Academic, New York, 1975).
[19]L. M. Milne-Thomson, *The Calculus of Finite Differences* (Macmillan, London, 1933).
[20]*Handbook of Mathematical Functions,* edited by M. Abramowitz and I. A. Stegun (Dover, New York, 1965).